HHS Public Access

Author manuscript

Angew Chem Int Ed Engl. Author manuscript; available in PMC 2020 April 08.

Published in final edited form as:

Angew Chem Int Ed Engl. 2020 February 10; 59(7): 2844–2849. doi:10.1002/anie.201912640.

Asymmetric Hydrogenation of Unfunctionalized Tetrasubstituted Acyclic Olefins

Raphael Bigler[*],
Pharmaceutical Division, Small Molecules Technical Development, Department of Process Chemistry and Catalysis, F. Hoffmann-La Roche Ltd, 4070 Basel (Switzerland)

Kyle A. Mack,
Department of Small Molecule Process Chemistry, Genentech, Inc., 1 DNA Way, South San Francisco, CA 94080 (USA)

Jeff Shen,
Department of Small Molecule Process Chemistry, Genentech, Inc., 1 DNA Way, South San Francisco, CA 94080 (USA)

Paolo Tosatti,
Pharmaceutical Division, Small Molecules Technical Development, Department of Process Chemistry and Catalysis, F. Hoffmann-La Roche Ltd, 4070 Basel (Switzerland)

Chong Han,
Department of Small Molecule Process Chemistry, Genentech, Inc., 1 DNA Way, South San Francisco, CA 94080 (USA)

Stephan Bachmann,
Pharmaceutical Division, Small Molecules Technical Development, Department of Process Chemistry and Catalysis, F. Hoffmann-La Roche Ltd, 4070 Basel (Switzerland)

Haiming Zhang[*],
Department of Small Molecule Process Chemistry, Genentech, Inc., 1 DNA Way, South San Francisco, CA 94080 (USA)

Michelangelo Scalone,
Pharmaceutical Division, Small Molecules Technical Development, Department of Process Chemistry and Catalysis, F. Hoffmann-La Roche Ltd, 4070 Basel (Switzerland)

Andreas Pfaltz,
Department of Chemistry, University of Basel, 4056 Basel (Switzerland)

Scott E. Denmark,
Roger Adams Laboratory, Department of Chemistry, University of Illinois, Urbana, IL 61801 (USA)

Stefan Hildbrand,

[*] raphael.bigler@roche.com, zhang.haiming@gene.com, gosselin.francis@gene.com.

Conflict of interest
The authors declare no conflict of interest.

Supporting information and the ORCID identification number(s) for the author(s) of this article can be found under: https://doi.org/10.1002/anie.201912640.

Pharmaceutical Division, Small Molecules Technical Development, Department of Process Chemistry and Catalysis, F. Hoffmann-La Roche Ltd, 4070 Basel (Switzerland)

Francis Gosselin*

Department of Small Molecule Process Chemistry, Genentech, Inc., 1 DNA Way, South San Francisco, CA 94080 (USA)

Abstract

Asymmetric hydrogenation has evolved as one of the most powerful tools to construct stereocenters. However, the asymmetric hydrogenation of unfunctionalized tetrasubstituted acyclic olefins remains the pinnacle of asymmetric synthesis and an unsolved challenge. We report herein the discovery of an iridium catalyst for the first, generally applicable, highly enantio- and diastereoselective hydrogenation of such olefins and the mechanistic insights of the reaction. The power of this chemistry is demonstrated by the successful hydrogenation of a wide variety of electronically and sterically diverse olefins in excellent yield and high enantio- and diastereoselectivity.

Keywords

asymmetric catalysis; hydrogenation; iridium; N,P ligands; tetrasubstituted olefins

Introduction

Over the past decades, the asymmetric hydrogenation of C=C, C=O, and C=N double bonds has matured to become one of the premier methods to install stereocenters in organic molecules, with several industrial processes relying on its chemical prowess.[1] Moreover, the awarding of half of the 2001 Nobel Prize in Chemistry for asymmetric hydrogenation is testament to its transformational impact on organic synthesis.[2] Among the most challenging substrates to date are unfunctionalized olefins, as they lack both nearby heteroatoms acting as transient coordinating groups to the metal center and polarity effects activating the double bond.[3] Whereas the reduction of 1,1-disubstituted and trisubstituted alkenes affords products with a single stereocenter, the asymmetric hydrogenation of tetrasubstituted olefins can generate two vicinal stereocenters and thus give rise to products of higher stereochemical complexity. Owing to the aforementioned reasons and the challenges associated with their steric encumbrance, unfunctionalized tetrasubstituted acyclic olefins arguably represent the most challenging substrate class for asymmetric hydrogenation.[4,5]

After an initial report by Buchwald on the asymmetric hydrogenation of unfunctionalized tetrasubstituted olefins using a highly electrophilic but sensitive ansa-zirconocene catalyst,[6] Pfaltz's application of iridium/phosphinyl oxazoline (PHOX) complexes[7] paved the way for the development of several related catalysts.[8,9] In all cases, the investigated substrates were restricted to simple cyclic 2,3-disubstituted indenes, 3,4-disubstituted 1,2-dihydronaphthalenes and, if acyclic, trimethylstyrenes (Figure 1). In most cases, the iridium catalysts show variable enantioselectivity and little functional group tolerance. Thus, while

considerable progress has been made for functionalized analogues,[5,10] the asymmetric hydrogenation of unfunctionalized tetrasubstituted acyclic olefins has remained an open challenge.

Recently, we disclosed efficient methods for the stereoselective synthesis of tetrasubstituted, acyclic olefins,[11] whose enantioselective reduction would give rise to intriguing structural motifs inaccessible with state-of-the-art synthetic methods. In this article, we report the first generally applicable, highly enantio- and diastereoselective hydrogenation of such unfunctionalized tetrasubstituted acyclic olefins.

Results and Discussion

(*E*)-2,3-Diphenylbut-2-ene ((*E*)-**2a**) was chosen as a representative starting point for our study (Figure 2). An initial parallel screening of a subset of 34 iridium catalysts in our catalyst library (see Figure S1 and Table S1 in the Supporting Information) led to rapid hit identification. The best-performing PHOX-type complex (*S*)-**1a**[7a] afforded the desired product (2*R*,3*R*)-**3a** in 80% conversion and a diastereomeric ratio (dr) of 98:2 under relatively mild conditions (2 mol% catalyst, 50 bar H_2, PhCl, 30°C, 24 h), albeit with a poor enantiomeric ratio (er) of 80:20. The modular synthetic approach to catalysts bearing such phosphinomethyl-oxazoline ligands allowed for efficient structure optimization and a secondary serial screening of 15 variants (see Figure S2 and Table S2 in the Supporting Information) identified (*R*)-**1o** as the optimal catalyst, now affording the desired product (2*S*,3*S*)-**3a** with >99% conversion, 98:2 dr and substantially improved enantioselectivity (98:2 er).

Catalyst (*R*)-**1o** proved highly successful in the hydrogenation of a broad range of substrates (Figure 3a). Both electron-donating and electron-withdrawing substituents could be incorporated on the (*E*)-1,2-dimethyl-1,2-diaryl olefin core ((*E*)-**2a–f,h**). Only the most electron-deficient alkene (*E*)-**2g** bearing two trifluoromethyl groups on the aryl substituents could not be hydrogenated successfully. The enantiomeric ratio of the major diastereomer remained high (>99:1–97:3 er), whereas the minor diastereomer showed low enantiomeric purity throughout (63:37–50:50 er). Crucially, several important functional groups such as Cl (**2i**), TMS (**2j**), Bpin (**2k**), $NHCOCF_3$ (**2l**), OAc (**2m**), CO_2Me (**2n**), OTIPS (**2o**) and OBn (**2p** and **2q**) were compatible and did not affect the efficacy of this transformation.

The substrate scope is not restricted to the (*E*)-1,2-dimethyl-1,2-diaryl substructure: several other (*E*)-1,2-dialkyl-1,2-diaryl olefins ((*E*)-**2r–y**), but also 1,1-dialkyl-2,2-diaryl olefins (**2z** and **2aa**) and very challenging alkyl-triaryl olefins (**2ae**–**ai**) were all hydrogenated with excellent yield, er, and dr. Importantly, catalyst (*R*)-**1o** provided optimal results for all tested substrates, thus obviating the need to build up large catalyst libraries often required for other iridium-based catalyst systems.[7a,8a] Low enantioselectivity was observed only for extremely challenging substrates, that is, in which the *Re*- and *Si*-faces are differentiated only by the electronic properties of the aromatic substituents ((*Z*)-**2c** and **2ac**) or the length of an alkyl substituent (**2ab**) as well as for trialkyl-aryl substrate **2ad**. In addition, both enantiomers of the catalyst are readily available. Thus, the application of (*R*)-**1o** and (*S*)-**1o** in the asymmetric hydrogenation of 1,1-dialkyl-2,2-diaryl olefins (*E*)-**2aj** and (*Z*)-**2aj**

allowed access to all four stereoisomers of the product **3aj** with outstanding stereoselectivities (Figure 3b).

The reaction was preparatively useful and readily scalable: the asymmetric hydrogenation of Bpin-containing olefin (*E*)-**2k** occurred with virtually the same efficiency on a gram scale (Figure 3c). This allowed for the preparation of (2*S*,3*S*)-**3k** and its use in different post-hydrogenation chemical modifications of interest to medicinal chemists,[13] highlighting the utility of this asymmetric hydrogenation protocol to introduce vicinal stereocenters in organic synthesis.

Although catalysts similar to (*R*)-**1o**, for example catalyst (*S*)-**1j** bearing a phenyl group instead of the 3,5-bis-*tert*-butylphenyl motif, have previously been reported by the Pfaltz group,[7a] the introduction of two *tert*-butyl groups has a substantial effect on the activity and selectivity of the catalyst, which is particularly pronounced for challenging substrates. For example, the hydrogenation of (*Z*)-**2aa** with (*R*)-**1o** occurs in 98% yield with 95:5 dr and 99:1 er. In contrast, its phenyl analogue (*S*)-**1j** achieves only 17% conversion with 91:9 dr and 97:3 er under otherwise identical conditions. Furthermore, employing analogue (*S*)-**1c** bearing diphenylphosphine and isopropyl oxazoline donors failed to give any of the desired product, whereas it was the catalyst of choice for cyclic tetrasubstituted olefins and trimethylstyrenes (see Table S3 in the Supporting Information for additional examples). These results clearly highlight the challenges associated with the hydrogenation of acyclic, tetrasubstituted olefins and the substantial improvement achieved by introducing a 3,5-bis-*tert*-butylphenyl motif on the oxazoline donor.

To shed light on the origin of diastereoselectivity, we conducted the hydrogenation of (*E*)-**2d** under D_2 atmosphere and observed incomplete deuterium incorporation at the benzylic positions as well as partial deuteration of the formerly allylic positions, indicating the possibility of a competing β-hydride elimination/reinsertion pathway (Figure 4a). This observation is particularly relevant for the formation of the minor diastereomer, in which only 55% D incorporation was observed at both benzylic positions. Although only a small kinetic isotope effect (KIE) was observed when the reaction was performed under D_2 vs. H_2 (k_H/k_D = 1.3), perdeuteration of the methyl groups in (*E*)-**2a** led to a considerable KIE of 2.0 in a competition experiment (Figure 4b). The increased KIE is potentially caused by the multiplicative effect of deuterium atoms,[14] underlining the non-innocence of the allylic hydrogens in the catalytic cycle. However, hydrogenation of the isomerized olefins **4a** favored the formation of *meso*-**3a**, thus showing that non-metalbound **4a** is not an intermediate in the main catalytic cycle (Figure 4c).

On the basis of previous studies on Ir-catalyzed hydrogenations, our experimental observations, and DFT calculations for the asymmetric hydrogenation of model substrate (*E*)-**2a** with catalyst (*R*)-**1o**, we propose a plausible mechanistic pathway (Figure 5) with a main Ir^{III}/Ir^{V} catalytic cycle in which the resting state of the catalyst is the Ir^{III} dihydride species **Ir-I**.[15,16] Endergonic coordination of (*E*)-**2a** to **Ir-I** leads to the formation of **Ir-II**. Subsequent endergonic coordination of **Ir-II** and H_2, followed by simultaneous hydride transfer (migratory insertion) and oxidative addition of H_2 generates Ir^{V} intermediate **Ir-III**. The enantioselectivity is dictated by the relative barriers of the hydride transfer/oxidative

addition step in accordance with the Curtin–Hammett principle. For this particular olefin–catalyst pairing, the experimental er (98:2) is in excellent agreement with the calculated relative energy difference of 2.3 kcalmol^{-1} (97:3 er). In a previous report, Bayer et al. suggested that the stereochemical outcome of a similar reaction is influenced by a key C–H/π dispersive interaction between the substrate aryl ring and the oxazoline moiety.[15e] Comparing TS1 and TS1′ (Figure 5), it is clear that there is a much more efficient overlap of the aryl ring with the oxazoline C–H moiety in TS1. Furthermore, to accommodate this interaction in TS1′, the 3,5-bis-*tert*-butylphenyl group must rotate away from the substrate, which causes a distortion in the ligand backbone due primarily to steric clash with the adjacent cyclohexane substituent. These powerful interactions are particularly prominent in the hydrogenation of tetrasubstituted olefins where the substrate cannot orient itself to place a vinyl hydrogen proximal to the oxazoline ring.

Reductive elimination of intermediate **Ir-III** affords the hydrogenated product (2*S*,3*S*)-**3a** and regenerates the Ir^{III} dihydride catalyst **Ir-I**. Intermediate **Ir-III** may also undergo a competitive β-hydride elimination and simultaneous reductive elimination of H_2 to give intermediate **Ir-IV**. The calculated energy barrier corresponds to a 98:2 preference for reductive elimination over the β-hydride elimination. Complex **Ir-IV** undergoes either H_2 coordination and oxidative addition/migratory insertion to produce **Ir-V**, which reductively eliminates leading to formation of product (2*S*,3*S*)-**3a**, or exchange of *Re*- and *Si*-bound olefin complexes by decomplexation/recomplexation to arrive at **Ir-IV′**.[15c] From **Ir-IV′**, a related sequence produces the minor diastereomer *meso*-**3a**.

Interestingly, performing the reaction with (*E*)-**2a** under 2 bar of H_2 (instead of 50 bar) still leads to full conversion and high er (99:1) but with significantly eroded dr (78:22). Calculations on an alternative Ir^{III}/Ir^{I} catalytic cycle (see the Supporting Information),[18] which was only +1.1 kcal mol^{-1} higher in energy than the proposed Ir^{III}/Ir^{V} cycle, exhibited high er (≫99:1) but an attenuated difference in energy between reductive elimination and β-hydride elimination (0.5 kcal mol^{-1}). Both mechanisms include intermediate **Ir-II** (Figure 6). However, while H_2 coordination is required in the Ir^{III}/Ir^{V} cycle, this intermediate undergoes direct hydride transfer (migratory insertion) in the Ir^{III}/Ir^{I} cycle to give Ir^{III} intermediate **Ir-VI**, which can reductively eliminate to give product and Ir^{I} species **Ir-VII**. Given these results, it is likely that a H_2 pressure-dependent shift in mechanism from Ir^{III}/Ir^{V} at high pressure to Ir^{III}/Ir^{I} at low pressure is operative, accounting for the reduced dr at lower pressure.

Conclusion

Asymmetric hydrogenation of olefins has been a heavily studied area for decades. However, despite recent advances, a general method for highly selective asymmetric hydrogenation of unfunctionalized tetrasubstituted acyclic olefins has remained elusive. In this report, we have developed a catalyst which allows for the first time to successfully hydrogenate these challenging substrates and we have also demonstrated its generality, scalability, and selectivity. We believe that this advance will have an important impact in catalysis and synthesis as it allows rapid access to complex structural motifs inaccessible with other state-of-the-art methods.

Experimental Section

A representative procedure for the asymmetric hydrogenation of unfunctionalized tetrasubstituted acyclic olefins is as follows. In a glove box, (*E*)-**2a** (20.8 mg, 100 μmol) and (*R*)-**1o** (3.3 mg, 2.00 μmol) are added to a 30 mL autoclave with a glass inset. PhCl (1.0 mL, degassed under Ar) is added to the mixture and the autoclave is sealed and removed from the glove box. The autoclave is connected to a H_2 line, flushed with H_2 (3 × 20 bar), and sealed under H_2 (50 bar). The autoclave is placed in a preheated metal block and the reaction is stirred at 30°C for 24 h. The pressure is released and the solvent is removed under reduced pressure. The crude reaction mixture is dissolved in TBME (1 mL) and filtered through a pad of silica gel with TBME (5 mL). The solvent is removed under reduced pressure and the product is analyzed by ^{1}H NMR, GC, and chiral HPLC. Full experimental details and characterization of the compounds are given in the Supporting Information.

Supplementary Material

Refer to Web version on PubMed Central for supplementary material.

Acknowledgements

We thank A. Alker, R. Santillo, P. Schmitt, A. Becht Joerger, I. Duffour, O. Fuchs, M. Buerkler, P. Cron, I. Plitzko, C. Wyss Gramberg, C. Bartelmus, S. Brogly, O. Scheidegger, J. Schneider and N. Valente for experimental and analytical support. We are grateful to the Roche Technology, Innovation and Science Committee for funding.

References

[1]. Püntener K, Scalone M in Asymmetric Catalysis on Industrial Scale (Eds.: Blaser H-U, Federsel H-L), Wiley-VCH, Weinheim, 2010, pp. 13–25.

[2]. a)Knowles WS, Angew. Chem. Int. Ed 2002, 41, 1998–2007; Angew. Chem. 2002, 114, 2096–2107;b)Noyori R, Angew. Chem. Int. Ed 2002, 41, 2008–2022; Angew. Chem. 2002, 114, 2108–2123.

[3]. a)Woodmansee DH, Pfaltz A, Chem. Commun 2011, 47, 7912–7916;b)Cui X, Burgess K, Chem. Rev 2005, 105, 3272–3296. [PubMed: 16159153]

[4]. Margarita C, Andersson PG, J. Am. Chem. Soc 2017, 139, 1346–1356. [PubMed: 28064490]

[5]. Kraft S, Ryan K, Kargbo RB, J. Am. Chem. Soc 2017, 139, 11630–11641. [PubMed: 28800391]

[6]. Troutman MV, Apella DH, Buchwald SL, J. Am. Chem. Soc 1999, 121, 4916–4917.

[7]. a)Schrems MG, Neumann E, Pfaltz A, Angew. Chem. Int. Ed 2007, 46, 8274–8276; Angew. Chem. 2007, 119, 8422–8424;b)Schrems MG, Neumann E, Pfaltz A, Heterocycles 2008, 76, 771–781.

[8]. a)Busacca CA, Qu B, Grět N, Fandrick KR, Saha AK, Marsini M, Reeves D, Haddad N, Eriksson M, Wu J-P, Grinberg N, Lee H, Li Z, Lu B, Chen D, Hong Y, Ma S, Senanayake CH, Adv. Synth. Catal 2013, 355, 1455–1463;b)Wassenaar J, Detz RJ, de Boer SY, Lutz M, van Maarseveen JH, Hiemstra H, Reek JNH, J. Org. Chem 2015, 80, 3634–3642; [PubMed: 25748824] c)Zanotti-Gerosa A, Gazić Smilović I, Časar Z, Org. Chem. Front 2017, 4, 2311–2322;d)Biosca M, Salomó ME, de la Cruz-Sánchez P, Riera A, Verdaguer X, Pàmies O, Diéguez M, Org. Lett 2019, 21, 807–811; [PubMed: 30648389] e)Biosca M, Magre M, Pàmies O, Diéguez M, ACS Catal. 2018, 8, 10316–10320.

[9]. For a rhodium catalyst, see:Zhang Z, Wang J, Li J, Yang F, Liu G, Tang W, He W, Fu J-J, Shen Y-H, Li A, Zhang W-D, J. Am. Chem. Soc 2017, 139, 5558–5567. [PubMed: 28271887]

[10]. a)Kerdphon S, Ponra S, Yang J, Wu H, Eriksson L, Andersson PG, ACS Catal. 2019, 9, 6169–6176;b)Ponra S, Rabten W, Yang J, Wu H, Kerdphon S, Andersson PG, J. Am. Chem. Soc 2018, 140, 13878–13883. [PubMed: 30265529]

[11]. a)Li BX, Le DN, Mack KA, McClory A, Lim N-K, Cravillion T, Savage S, Han C, Collum DB, Zhang H, Gosselin F, J. Am. Chem. Soc 2017, 139, 10777–10783; [PubMed: 28715208] b)Mack KA, McClory A, Zhang H, Gosselin F, Collum DB, J. Am. Chem. Soc 2017, 139, 12182–12189; [PubMed: 28786667] c)Savage S, McClory A, Zhang H, Cravillion T, Lim N-K, Masui C, Robinson SJ, Han C, Ochs C, Rege PD, Gosselin F, J. Org. Chem 2018, 83, 11571–11576; [PubMed: 30200756] d)Lim N-K, Weiss P, Li BX, McCulley CH, Hare SR, Bensema BL, Palazzo TA, Tantillo DJ, Zhang H, Gosselin F, Org. Lett 2017, 19, 6212–6215; [PubMed: 29115843] e)Lim N-K, Cravillion T, Savage S, McClory A, Han C, Zhang H, DiPasquale A, Gosselin F, Org. Lett 2018, 20, 1114–1117. [PubMed: 29397753]

[12]. Details of the crystallographic analyses are given in the Supporting Information. CCDC 1969737 and 1969736 [(2*S*,3*S*)-**3k** and (1*S*,2*S*)-**3ah**, respectively] contain the supplementary crystallographic data for this paper. These data can be obtained free of charge from The Cambridge Crystallographic Data Centre.

[13]. a)Vantourout JC, Miras HN, Isidro-Llobet A, Sproules S, Watson AJB, J. Am. Chem. Soc 2017, 139, 4769–4779; [PubMed: 28266843] b)Armstrong RJ, Niwetmarin W, Aggarwal VK, Org. Lett 2017, 19, 2762–2765; [PubMed: 28453280] c)Fawcett A, Biberger T, Aggarwal VK, Nat. Chem 2019, 11, 117–122; [PubMed: 30532013] d)Myhill JA, Zhang L, Lovinger GJ, Morken JP, Angew. Chem. Int. Ed 2018, 57, 12799–12803; Angew. Chem. 2018, 130, 12981–12985.

[14]. Streitwieser A, Jagow RH, Fahey RC, Suzuki S, J. Am. Chem. Soc 1958, 80, 2326–2332.

[15]. a)Fan Y, Cui X, Burgess K, Hall MB, J. Am. Chem. Soc 2004, 126, 16688–16689; [PubMed: 15612683] b)Church TL, Rasmussen T, Andersson PG, Organometallics 2010, 29, 6769–6781;c)Hopmann KH, Bayer A, Organometallics 2011, 30, 2483–2497;d)Sparta M, Riplinger C, Neese F, Chem J. Theory Comput. 2014, 10, 1099–1108;e)Hopmann KH, Fredani L, Bayer A, Organometallics 2014, 33, 2790–2797;f)Gruber S, Pfaltz A, Angew. Chem. Int. Ed 2014, 53, 1896–1900; Angew. Chem. 2014, 126, 1927–1931.

[16]. We also surveyed alternative mechanisms including Ir^{I}/Ir^{III} and additional Ir^{III}/Ir^{V} pathways, which are included and discussed in the Supporting Information.

[17]. CYLview, 1.0b; C. Y. Legault, Université de Sherbrooke, 2009 (http://www.cylview.org).

[18]. Dietiker R, Chen P, Angew. Chem. Int. Ed 2004, 43, 5513–5516; Angew. Chem. 2004, 116, 5629–5632.

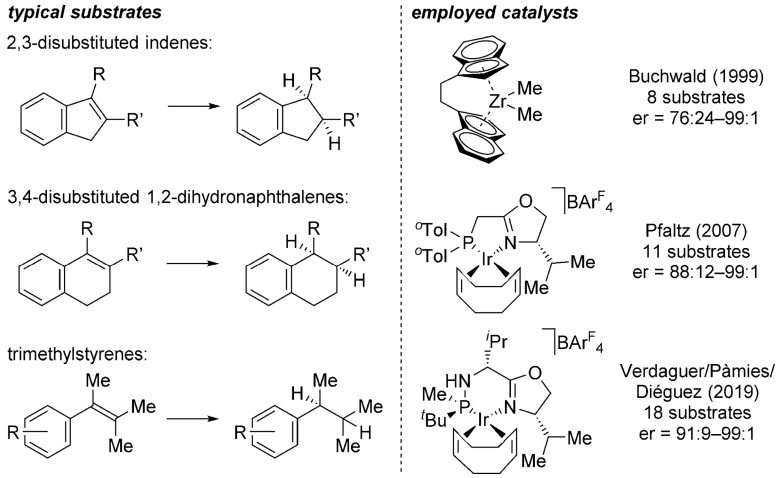

Figure 1.

Commonly investigated substrates and state-of-the-art catalysts. Ar^F = 3,5-bis(trifluoromethyl)phenyl; ^{o}Tol=*ortho*-tolyl.

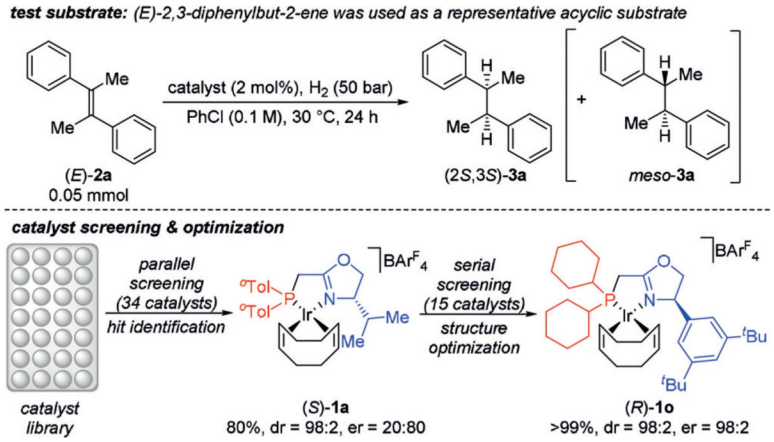

Figure 2.

Catalyst screening and optimization for the asymmetric hydrogenation of (*E*)-**2a** (conversion to product is reported). (*S*)-**1a** and (*R*)-**1o** afford opposite enantiomers of **3a**.

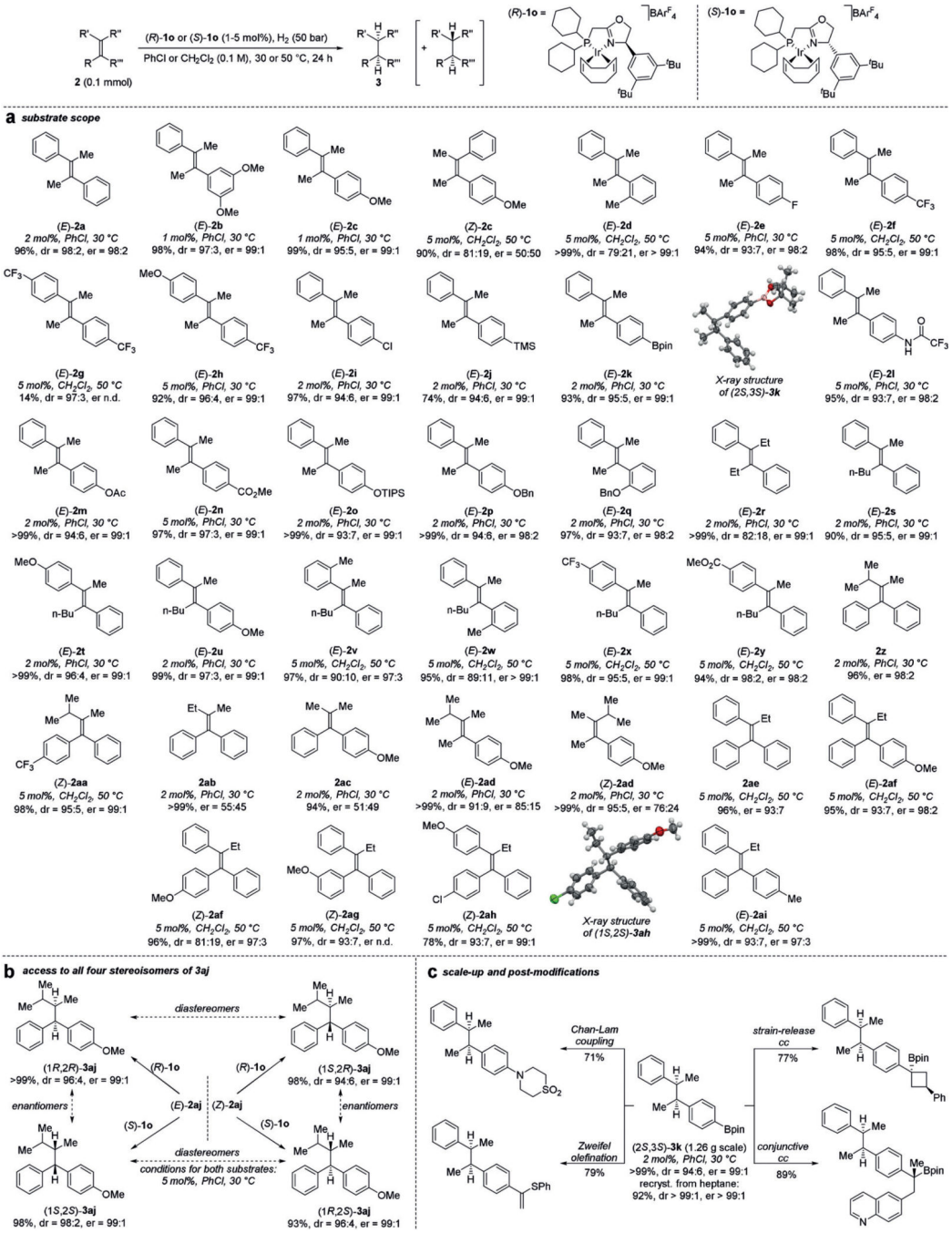

Figure 3.

Ir-catalyzed asymmetric hydrogenation of unfunctionalized tetrasubstituted acyclic olefins. The general reaction scheme is shown at the top. a,b) Yields of isolated products are reported (except for (2*S*,3*S*)-**3g**); dr and er (major diastereomer) are obtained from the crude reaction mixtures after filtration through silica gel. Absolute configurations of products are assigned in analogy to (2*S*,3*S*)-**3k** and (1*S*,2*S*)-**3ah**, for which it was determined by X-ray crystallography.[12] c) Scale-up of the synthesis of (2*S*,3*S*)-**3k** at 1.26 g (3.8 mmol) and post-modifications (see the Supporting Information for details) of (2*S*,3*S*)-**3k**. Yields of isolated

post-modification products are shown (dr>20:1 for all isolated products). Ac=acetyl; Bn=benzyl; pin=pinacolato; TIPS=triisopropylsilyl; TMS=trimethylsilyl.

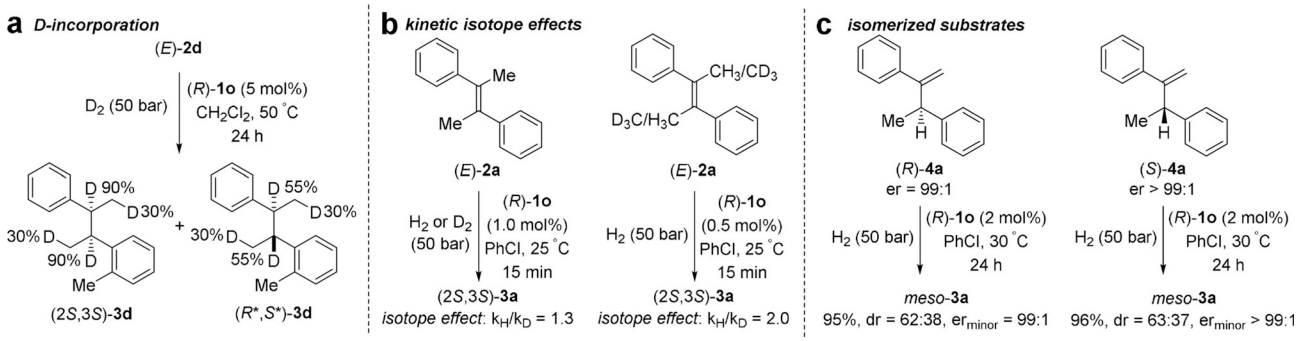

Figure 4.

Mechanistic experiments. a) Deuterium incorporation in asymmetric hydrogenation (AH) of (*E*)-**2d**. b) Kinetic isotope effects in AH of (*E*)-**2a**. c) AH of isomerized compounds **4a**. AH of (*R*)-**4a** and (*S*)-**4a** affords (*S,S*)-**3a** and (*R,R*)-**3a** as the minor diastereomer, respectively.

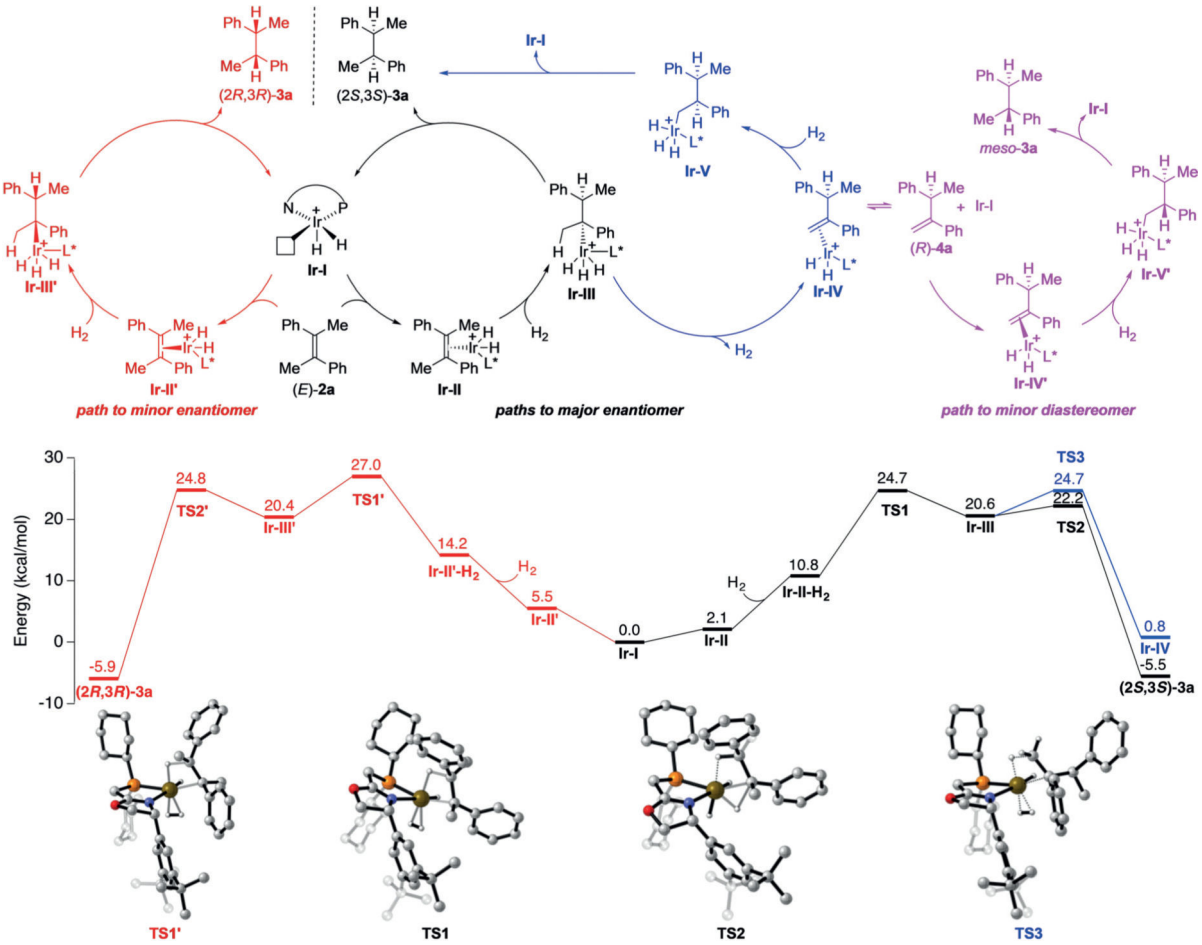

Figure 5.

Catalytic cycle, which includes provisions for the formation of (2*S*,3*S*)-**3a** (black and blue), minor enantiomer (2*R*,3*R*)-**3a** (red), and diastereomer *meso*-**3a** (violet). Gibbs free energies for relevant ground state and transition state structures of the proposed catalytic cycle and 3D representations of key transition states along the reaction coordinate.[17] See the Supporting Information for more details.

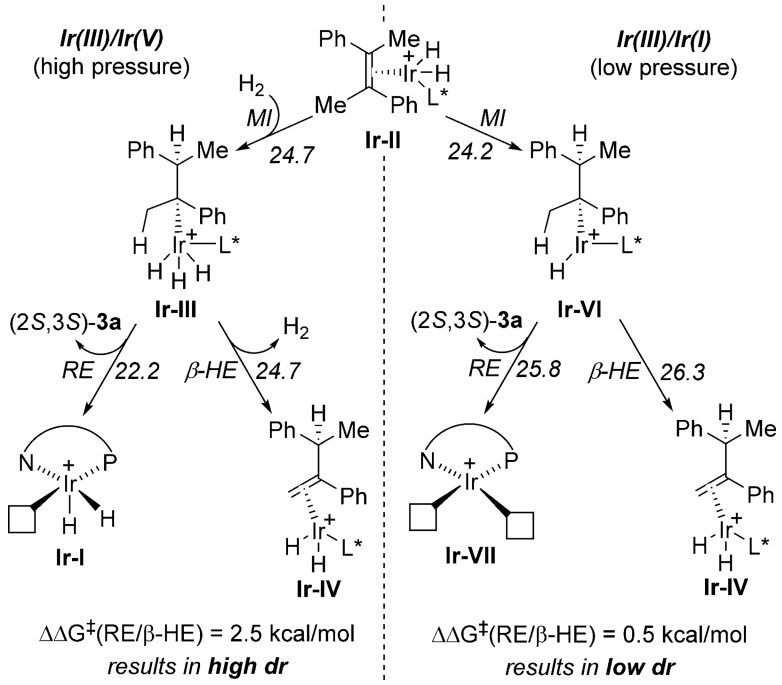

Figure 6.
Pressure-dependent shift of mechanism.